Diffusion Tensor Tract Analysis of Patients with Traumatic Brain Injury: Stratification by Susceptibility Weighted Imaging

A H Bauer, S D Weiss, K Nael, H Fisk, B D Pressman, F G Moser

Citation

A H Bauer, S D Weiss, K Nael, H Fisk, B D Pressman, F G Moser. *Diffusion Tensor Tract Analysis of Patients with Traumatic Brain Injury: Stratification by Susceptibility Weighted Imaging*. The Internet Journal of Radiology. 2018 Volume 21 Number 1.

DOI: 10.5580/IJRA.53577

Abstract

Traumatic brain injury (TBI) can damage white matter resulting in neurological impairments. Diffusion tensor imaging (DTI) may be a more sensitive technique than conventional magnetic resonance imaging (MRI) in assessing TBI. The purpose of this study was to determine whether presence of microhemorrhage on susceptibility weighted imaging (SWI) could be a determining factor in quantitative DTI tractography in patients with prior TBI. In this retrospective study, 57 patients with history of TBI underwent 3.0T MRI including DTI and SWI: (A) 27 patients with demonstrable microhemorrhages on SWI (SWI(+)) and (B) 30 with normal SWI (SWI(-)). The control group comprised 29 subjects from a normative database. Multimodal analysis including atlas-based tractography was performed generating average fractional anisotropy (FA), mean diffusivity (MD), and voxel number (VN) for 6000 tracts. ANCOVA and receiver-operating characteristic (ROC) analysis determined the optimal parameters, connection tracts, and thresholds for predicting TBI. FA was increased in tracts connecting the basal ganglia and cortex and decreased in tracts within the frontal lobe in trauma patients vs. controls ($P < .05$). VN was decreased in 13 tracts and 9 tracts showed increased VN with FA in trauma patients vs. controls ($P < .05$). The best diagnostic power distinguishing trauma from control was obtained using FA and VN values in 4 tracts, yielding area under the curve of 0.93 and sensitivity/specificity of 85/86%. With its ability to differentiate TBI patients from controls, diffusion-tensor tractography is a promising technique in identifying white matter structural changes of chronic TBI not imaged by conventional MRI.

INTRODUCTION

Traumatic brain injury (TBI) is a prevalent public healthcare problem with 2.4 million emergency department visits, hospitalizations, or fatalities in 2010.1 TBI can damage white matter tracts resulting in memory impairment, attention deficit, and headaches.2, 3, 4 Traumatic axonal injury, axonal damage as a result of shear-strain forces,5-7 is believed to be the cause of these neurological and cognitive impairments.8

While fluid attenuated inversion recovery, diffusion weighted imaging, and gradient echo imaging have traditionally been utilized for the identification of traumatic axonal injury, susceptibility weighted imaging (SWI) has been shown to increase sensitivity, identifying tiny microhemorrhages otherwise undetectable with conventional MR imaging sequences.9,10,11,12 Likewise, diffusion tensor imaging (DTI) has been suggested to be sensitive in the detection of white matter injury with many studies investigating fractional anisotropy (FA) as a biomarker of TBI. Further, several studies have demonstrated correlation of lesions on DTI with cognitive performance.13-18 Recently, quantitative tractography, a method of performing diffusion tensor imaging analysis allowing calculation of FA and other diffusion tensor parameters averaged over the selected fiber tract, has shown utility in improving the diagnostic accuracy in patients with TBI and normal findings on routine MR images.19

The purpose of this study was to determine whether presence of microhemorrhage on SWI can be a determining factor in DTI tract analysis in patients with prior head trauma and to evaluate the diagnostic power of quantitative tractography in identifying SWI negative chronic brain trauma. Specifically, the aim was to determine whether there are changes in the diffusion characteristics and volume of the white matter tracts by performing a DTI tract analysis in SWI(+) and SWI(-) patients with prior TBI and in comparison with normal healthy controls without TBI.

METHODS

Participants.

This retrospective study was approved by the Institutional Review Board. From 2012 to 2014, 78 patients underwent 3.0 T MRI for the evaluation of TBI. Patients were included in this study if (a) they had a history of remote trauma (6-12 months prior); (b) they were between 20 and 60 years old (to limit the effect of changes in FA with age); (c) they had no history of other neurologic or vascular disease, chronic hypertension, or chronic alcoholism; (d) they had no findings of brain disease on conventional MRI including findings of trauma such as encephalomalacia or white matter disease (e) they had five or less microhemorrhages on SWI. The results were compared with 29 healthy control subjects (normative database) neither history of trauma as verified in the hospital electronic medical record nor any abnormalities on MRI of the brain.

Image acquisition.

All patients underwent MR imaging on a 3T Siemens Verio MR imaging system (Siemens, Erlangen, Germany) with a 12-channel phased array head coil. TBI protocol consisted of the following sequences: axial T1-weighted MPRAGE (TE = 2.96 ms, TR = 2100 ms, FA = 9°, [FOV] = 230 mm, matrix = 256, slice thickness = 1.2 mm, slice gap = 0.6 mm, image scan time ~ 5 min), axial FLAIR (TE = 89 ms, TR = 9000 ms, TI = 2500 ms, [FOV] = 230 mm, matrix = 320, slice thickness = 4 mm, slice gap = 1 mm, image scan time ~ 5 min), axial T2-weighted TSE (TE = 97 ms, TR = 6000 ms, [FOV] = 230 mm, matrix = 512, slice thickness = 4 mm, slice gap = 1 mm, image scan time ~ 5 min), axial diffusion weighted TSE EPI (TE = 100 ms, TR= 6500 ms, [FOV] = 230 mm, matrix = 128, slice thickness = 4 mm, slice gap = 1 mm, image scan time ~ 2 min), axial SWI (TE = 20 ms, TR = 27 ms, FA = 15°, [FOV] = 230 mm, matrix = 320, slice thickness = 2 mm, slice gap = 0.4 mm, image scan time ~ 4 min), and DTI (TR = 6500 ms, TE = 100 ms, FOV = 240 mm, matrix = 128, slice thickness = 3.0 mm, 20 directions; diffusion- weighted factor, b = 700 s/mm2). No MRI acquisitions were repeated.

Image analysis, post processing and tractography.

A single board-certified subspecialty certified neuroradiologist reviewed the conventional MRI to exclude subjects with findings of TBI and studies corrupted by motion, and assessed SWI for the presence and number of microhemorrhages. BrainSuite © software, version 14c, was then utilized for all image post-processing: automated co-registration, cortical extraction, multimodal region of interest (ROI) segmentation, geometric distortion correction, and quantitative diffusion tensor tractography. For more details, please see: http://brainsuite.org/.

Quantitative tractography parameters were as follows: track seeding = 0.5 seeds/voxel, stepsize = 0.25 mm, angle threshold = 20 degrees [0,90], FA threshold = 0.25 [0,1], and length threshold = 100 mm. Tractconnect MATLAB function (http://neuroimage.usc.edu/neuro/Resources/TractConnect) was then implemented to generate mean FA, mean mean diffusivity (MD), and voxel number (VN) for 6000 connection tracts between 330 ROIs per brain. Of the 6000 connection tracts calculated per brain, only those present in all subjects were included for statistical analysis.

Statistical analysis.

Statistical analysis was performed by using Matlab version 2015b Statistics and Machine Learning Toolbox™ and MedCalc for Windows, Version 14.12.0 (MedCalc Software, Mariakerke, Belgium). A two-way ANOVA was calculated with the independent variables of HISTORY OF TRAUMA and SWI POSITIVITY (presence or absence of microhemorrhages) and the dependent variable, FA, MD, or VN. Two-way ANOVA was performed for each connection tract to identify the tracts with the greatest statistical difference of each parameter between SWI(+), SWI(-), and controls. Bartlett test was performed to ensure homogeneity of variances ($p > 0.05$). Subsequent two-way ANCOVA was then performed on those tracts found to be statistically significant by two-way ANOVA to control for the covariate, AGE. Levene's test was performed to ensure homogeneity of variances ($p > 0.05$). For interactions and main effects post-hoc paired comparisons testing (simple main effects analysis) took place. They were corrected using the Bonferroni method. Logistic regression analysis was performed to identify the contribution of each connection tract parameter to the model. Receiver operating characteristic (ROC) analysis was performed to ascertain the optimal connection tract parameters and threshold for determination of Trauma versus control, SWI(+) versus control, and SWI(-) versus control. Optimal thresholds were calculated for each ROC curve to maximize both sensitivity and specificity employing the Youden statistic. Subsequently, an ROC curve for the combination of parameters was calculated, extrapolating from the maximum-likelihood estimation model of combining classifiers 20. Area under the curve (AUC) was calculated for each individual tract's ROC curve as well as for the combined ROC curves. $P < 0.05$ was considered to indicate a statistically significant difference.

RESULTS

Of the 107 patients, 86 patients with a mean age of 36.4 were included: 27 patients with history of TBI and microhemorrhages (SWI(+)) (mean age ± SD: 34 years ± 11), 30 patients with history of TBI and without microhemorrhages (SWI(-)) (mean age ± SD: 34 years ± 9), and 29 patients from a normative database (Control) (mean age ± SD: 40 years ± 9). MRI images in 21 of the patients demonstrated findings of moderate or severe trauma or greater than 5 microhemorrhages on SWI and these patients were therefore excluded from the study.

Of the 6000 tracts calculated per brain, 613 were common to all subjects. Of the 27 patients demonstrating microhemorrhages, mean number of microhemorrhages was 3 ± 1. Locations of microhemorrhages included left and/or right superior, middle, inferior, orbitofrontal, and opercular frontal lobe, anterior, superior, middle and inferior temporal lobe, insula, parahippocampus, postcentral and angular parietal lobe, corona radiata, centrum semiovale, genu and splenium of the corpus callosum, and uncus.

SWI(+) vs. Control

No statistically significant difference was found in tract total average for any of the parameters including VN. Nine tracts demonstrated statistically significant differences in FA, 12 tracts in MD, and 14 tracts in VN. Classifiers with statistically significant differences within the ANCOVA model ($P \leq 0.02$) and between SWI(+) subjects and controls ($P \leq 0.05$) are tabulated in Table 1 with their corresponding means ± SD.

SWI(-) vs. Control

No statistically significant difference was found in tract total average for any of the parameters including VN. Sixteen tracts demonstrated statistically significant differences in FA, 13 tracts in MD, and 33 tracts in VN. Classifiers with statistically significant differences within the ANCOVA model ($P \leq 0.02$) and between SWI(-) subjects and controls ($P \leq 0.05$) are tabulated in Table 1 with their corresponding means ± SD.

SWI(+) vs. SWI(-)

Two tracts demonstrated statistically significant differences in FA, 0 tracts in MD, and 9 tracts in VN. Classifiers with statistically significant differences within the ANCOVA model ($P \leq 0.02$) and between SWI(+) subjects and SWI(-) subjects ($P \leq 0.05$) are tabulated in Table 1 with their corresponding means ± SD.

Trauma (SWI(+) and SWI(-)) vs. Control

No statistically significant difference was found in tract total average for any of the parameters, including VN. Fifty-four tracts demonstrated statistically significant differences in FA, 53 tracts in MD, and 96 tracts in VN. Tracts with statistically significant differences between Trauma and Controls in greater than one classifier are provided in Table 2 with their corresponding means ± SD.

Logistic regression analysis utilizing the 22 tract classifiers with the most statistically significant differences between Trauma and Control ($P \leq 0.01$) yielded significant contribution from four tract classifiers listed in Table 2: Left globus pallidus – Brainstem (P=0.0003, 95% CI, 1.4 – 3.0), Left putamen - Left posterior orbitofrontal gyrus (P = 0.0007, 95% CI, 0.48 – 0.82), Right pars opercularis - Right postcentral gyrus (P = 0.0024, 95% CI, 0.91 – 0.98), Left middle temporal gyrus - Left inferior temporal gyrus (P=0.013; 95% CI, 1.0-1.3). Optimal threshold values, area under the curve, and corresponding sensitivity and specificity for the combination of these four classifiers in the differentiation of Trauma versus Control are summarized in Table 3 with corresponding ROC curves provided in Figure 1.

Figure 1

ROC Curves

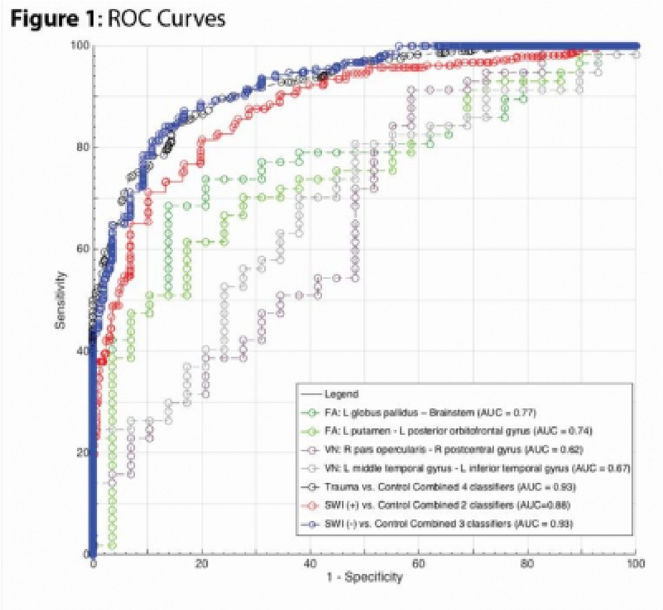

Table 1

ANCOVA

TABLE 1: ANCOVA

	ROI1	ROI2	Fiber Tract	SWI (-) mean	SE	SWI (+) mean	SE	Control mean	SE	ANCOVA P-value	SWI (+) vs. SWI (-) P-value	SWI (+) vs. Control P-value	SWI (-) vs. Control P-value
Fractional Anisotropy	Left putamen	Left posterior orbito-frontal gy	Uncinate fasciculus	[illegible]	[illegible]	[illegible]	[illegible]	[illegible]	[illegible]	[illegible]	[illegible]	[illegible]	[illegible]
	Left putamen	Brainstem	Nigrostriatal	[illegible]	[illegible]	[illegible]	[illegible]	[illegible]	[illegible]	[illegible]	[illegible]	[illegible]	[illegible]
	Right middle temporal gyrus	Right superior temporal gyrus	Uncinate fasciculus	[illegible]	[illegible]	[illegible]	[illegible]	[illegible]	[illegible]	[illegible]	[illegible]	[illegible]	[illegible]
	Left pre-cuneus	Right cingulate gyrus	Cingulum	[illegible]	[illegible]	[illegible]	[illegible]	[illegible]	[illegible]	[illegible]	[illegible]	[illegible]	[illegible]
Voxel number	Right globus pallidus	Brainstem	Pallidotegmental fasciculus	[illegible]	[illegible]	[illegible]	[illegible]	[illegible]	[illegible]	[illegible]	[illegible]	[illegible]	[illegible]
	Right putamen	Right post-central gyrus	Cingulum	[illegible]	[illegible]	[illegible]	[illegible]	[illegible]	[illegible]	[illegible]	[illegible]	[illegible]	[illegible]
	Left temporal pole	Left middle temporal gyrus	Uncinate fasciculus	[illegible]	[illegible]	[illegible]	[illegible]	[illegible]	[illegible]	[illegible]	[illegible]	[illegible]	[illegible]
	Right superior temporal gyrus	Right middle temporal gyrus	Uncinate fasciculus	[illegible]	[illegible]	[illegible]	[illegible]	[illegible]	[illegible]	[illegible]	[illegible]	[illegible]	[illegible]
	Cerebellum	Left pre-central gyrus	Rubrospinal, IC, thalamic projections, superior cerebellar	[illegible]	[illegible]	[illegible]	[illegible]	[illegible]	[illegible]	[illegible]	[illegible]	[illegible]	[illegible]
	Right middle frontal gyrus	Right pre-central gyrus	SLF	[illegible]	[illegible]	[illegible]	[illegible]	[illegible]	[illegible]	[illegible]	[illegible]	[illegible]	[illegible]
	Right supramarginal gyrus	Right middle temporal gyrus	Uncinate fasciculus, [illegible]	[illegible]	[illegible]	[illegible]	[illegible]	[illegible]	[illegible]	[illegible]	[illegible]	[illegible]	[illegible]
Mean Diffusivity	Left putamen	Left post-central gyrus	Cingulum	[illegible]	[illegible]	[illegible]	[illegible]	[illegible]	[illegible]	[illegible]	[illegible]	[illegible]	[illegible]
	Cerebellum	Right paracentral lobule	Rubrospinal, IC, thalamic projections, superior cerebellar	[illegible]	[illegible]	[illegible]	[illegible]	[illegible]	[illegible]	[illegible]	[illegible]	[illegible]	[illegible]
	Right putamen	Right post-central gyrus	Cingulum	[illegible]	[illegible]	[illegible]	[illegible]	[illegible]	[illegible]	[illegible]	[illegible]	[illegible]	[illegible]
	Right amygdala	Right temporal pole	Uncinate fasciculus	[illegible]	[illegible]	[illegible]	[illegible]	[illegible]	[illegible]	[illegible]	[illegible]	[illegible]	[illegible]
Both FA (1) & VN (2)	(1) Left globus pallidus	Brainstem	Internal capsule/CST	[illegible]	[illegible]	[illegible]	[illegible]	[illegible]	[illegible]	[illegible]	[illegible]	[illegible]	[illegible]
	(2)			[illegible]	[illegible]	[illegible]	[illegible]	[illegible]	[illegible]	[illegible]	[illegible]	[illegible]	[illegible]
	(1) Right putamen	Brainstem	Internal capsule/CST	[illegible]	[illegible]	[illegible]	[illegible]	[illegible]	[illegible]	[illegible]	[illegible]	[illegible]	[illegible]
	(2)			[illegible]	[illegible]	[illegible]	[illegible]	[illegible]	[illegible]	[illegible]	[illegible]	[illegible]	[illegible]

Table 2

Trauma vs. Control ANCOVA

		Region1	Region2	Fiber Tract	Trauma mean	SE	Control mean	SE	P-value
FA (1) and VN (2) increase	(1)	Left globus pallidus	Brainstem	Pallidotegmental fasciculus	0.494	0.003	0.472	0.004	0.0001
	(2)				14759	818	10073	1146	0.001
	(1)	Left putamen	Left globus pallidus	Striatopallidal	0.478	0.003	0.463	0.004	0.01
	(2)				17405	961	12418	1347	0.003
	(1)	Right globus pallidus	Brainstem	Pallidotegmental fasciculus	0.494	0.003	0.479	0.005	0.01
	(2)				14676	817	9914	1146	0.001
	(1)	Right putamen	Brainstem	Nigrostriatum	0.498	0.003	0.477	0.004	0.0001
	(2)				11702	722	7813	1012	0.001
	(1)	Right putamen	Right globus pallidus	Striatopallidal	0.479	0.003	0.461	0.005	0.002
	(2)				17331	944	13131	1323	0.01
FA (1) and VN (2) decrease	(1)	Left middle temporal gyrus	Left middle occipital gyrus	Superior longitudinal fasciculus	0.432	0.004	0.447	0.006	0.04
	(2)				1815	157	2484	220	0.02
	(1)	Left putamen	Left posterior orbito-frontal	Cingulum	0.468	0.004	0.493	0.006	0.001
	(2)				2907	281	4239	394	0.01
	(1)	Left temporal pole	Left middle temporal gyrus	Inferior longitudinal	0.430	0.005	0.454	0.007	0.01
	(2)				989	125	1624	175	0.004
	(1)	Right putamen	Right posterior orbito-frontal	Cingulum	0.462	0.006	0.488	0.008	0.02
	(2)				3016	314	4211	441	0.03
FA (1) decrease and MD (3) increase	(1)	Left pre-cuneus	Right cingulate gyrus	Corpus callosum, cingulum	0.480	0.006	0.510	0.008	0.03
	(3)				761	5	744	7	0.04
VN (2) and MD (3) increase	(2)	Cerebellum	Left pre-central gyrus	Rubrospinal, IC, thalamic projections, superior cerebellar peduncle, CST	6510	276	5383	387	0.02
	(3)				691	3	678	4	0.01
	(2)	Right superior temporal gyrus	Right middle temporal gyrus	Inferior longitudinal	3173	214	2383	300	0.04
	(3)				751	4	737	6	0.04
	(2)	Cerebellum	Right paracentral lobule	Rubrospinal, IC, thalamic projections, superior cerebellar peduncle, CST	6076	337	4659	472	0.02
	(3)				698	3	681	4	0.001
	(2)	Cerebellum	Right pre-central gyrus	Rubrospinal, IC, thalamic projections, superior cerebellar peduncle, CST	6078	244	4906	341	0.01
	(3)				689	3	676	4	0.01
VN (2) decrease and MD (3) increase	(2)	Left thalamus	Brainstem	CST	9982	867	13819	1215	0.01
	(3)				729	5	710	7	0.02
	(2)	Right thalamus	Brainstem	CST	8750	835	12167	1171	0.02
	(3)				739	5	715	8	0.01
	(2)	Right thalamus	Right post-central gyrus	CST	2569	185	3595	259	0.002
	(3)				732	3	719	5	0.04
	(2)	Right thalamus	Right pre-central gyrus	CST	4006	243	5031	341	0.02
	(3)				701	3	691	4	0.05
FA (1), VN (2), and MD (3)	(1)	Left putamen	Brainstem	Nigrostriatum	0.495	0.003	0.476	0.004	0.001
	(2)				11914	737	8172	1033	0.004
	(3)				710	3	699	5	0.04
	(1)	Right putamen	Right post-central gyrus	Cingulum	0.473	0.004	0.451	0.006	0.01
	(2)				4112	241	2669	337	0.001
	(3)				701	3	684	4	0.001
Logistic Regression Parameters									
FA		Left globus pallidus	Brainstem	Pallidotegmental fasciculus	0.494	0.003	0.472	0.004	0.0001
		Left putamen	Left posterior orbito-frontal	Uncinate fasciculus	0.468	0.004	0.493	0.006	0.001
VN		Right pars opercularis	Right post-central gyrus	Superior longitudinal	1818	126	1189	177	0.005
		Left middle temporal gyrus	Left inferior temporal gyrus	Inferior longitudinal	6262	300	7799	420	0.004

Table 3

ROC Analysis

Table 3: ROC Analysis

	Classifier	Threshold Values	Sensitivity (%)	Specificity (%)	Area Under the Curve
Trauma vs. Control	1. FA: Left globus pallidus - Brainstem	0.49	0.74	0.79	0.77
	2. FA: Left putamen - Left posterior orbitofrontal gyrus	0.48	0.70	0.72	0.74
	3. VN: Right pars opercularis - Right postcentral gyrus	7699	0.39	0.79	0.62
	4. VN: Left middle temporal gyrus - Left inferior temporal gyrus	1265	0.70	0.62	0.67
	Combined 4 classifiers	0.49, 0.50, 3719, 2472	0.85	0.86	0.93
SWI (+) vs. Control	Combined 2 classifiers	0.50, 0.49	0.81	0.80	0.88
SWI (-) vs. Control	Combined 3 classifiers	0.49, 0.51, 2167	0.84	0.87	0.93

Abbreviations: AUC – area under the curve; FA – fractional anisotropy; ROC – receiver operating characteristic; SWI – susceptibility weighted imaging; VN – voxel number

DISCUSSION

In the current study, by using SWI imaging as a surrogate biomarker of TBI12 and automated tractography atlas-based spatial statistical software, we demonstrated that DTI tractography detects chronic white matter changes in patients with a history of TBI. We highlight several notable points:

The presented investigation adds clarification to the mounting evidence indicating DTI has the capability to detect chronic microstructural white matter alterations that result from TBI.13,14,16,19,21-35 As demonstrated in multiple prior studies of chronic TBI,13,14,16,19,21-35 there was decreased FA and/or increased MD in the superior longitudinal fasciculus, uncinate fasciculus, inferior longitudinal fasciculus, cingulum bundle, corpus callosum, internal capsule and corticospinal tracts. With the exception of two studies19,28 that utilized SWI for exclusion criteria, the majority of prior investigations looking at DTI measures in chronic TBI, used a T2*/GRE sequence to identify the presence of microhemorrhages in order to either include or exclude subjects or as a marker of traumatic axonal injury. Therefore, it is plausible that these studies may have underestimated the presence of microhemorrhage due to lower sensitivity of GRE compared to SWI in patients with TBI.11 Considering that microhemorrhages may lead to difficulties analyzing DTI parameters in white matter tracts because of susceptibility effects, 36,37 one may assume that the reported reduced FA and increased MD of white matter tracts in TBI patients27 in studies utilizing GRE and not SWI may have been confounded by an underestimation of microhemorrhages. However, in our study, both SWI(+) and SWI(-) cohorts demonstrated similar shifts in FA and VN of select white matter tracts when compared to patients with no history of trauma. Further, some of these same tracts demonstrated a persistent significant difference between Trauma (SWI(+) and SWI(-) grouped together) and controls. This not only suggests that the results of the prior studies without SWI are less likely to be confounded, but also provides further support for the conclusion that DTI has the ability to detect white matter changes of TBI not detected with SWI,19,28 and therefore, the capacity to identify injury before thought to be either not present or undetectable.

While the majority of the prior studies report either decreased or no change in FA in chronic TBI, our investigation also identified tracts with increased FA, many oriented in the craniocaudal direction. Though a counterintuitive finding, a few studies have also found increased FA attributing this to diminished crossing fibers leading to increased axonal packing.28,38 However, many of the tracts with increased FA in the present study extended from the striatum to the brainstem, regions with relatively less crossing fibers (compared to regions like the corona radiata). Further, there were no significant decreases in FA of tracts that would be assumed to be crossing these regions. Another potential explanation for increased FA is increased myelination. Yet, increases in myelination would be contrary to the previous finding of decreased white matter volume of patients with chronic TBI, 39 albeit in a different region. Still, alternative reasons for increased FA include microscopic deficits of axonal structures or decreases in axonal diameter, packing density, and branching.40 Aside from the theoretical causes of increased FA, what is clear is that the presented results suggest an alteration in the DTI streamlines in brains of patients with a history of TBI compared to those without history of TBI, perhaps in response to TBI, in regions implicated in chronic TBI according to the biomechanical model of concussion41 (nigrostriatal tract and pallidotegmental fasciculus coursing through the brainstem) as well as in locations established in prior studies (superior longitudinal fasciculus, uncinate fasciculus, inferior longitudinal fasciculus, cingulum bundle, corpus callosum, internal capsule and corticospinal tracts). Conceivably, in response to injury to neuronal fibers, the brain may strengthen certain pathways and weaken others to compensate long term. Similar findings have been shown in studies of psychiatric disorders42 possibly related to TBI.43

A curious finding was that VN showed significant increases with significant FA increases. VN is a measure of the volume of white matter corresponding to a distinct fiber bundle that exceeds the given FA threshold.44 VN and FA are inherently linked via the FA tracking threshold. Indeed, partial volume effects may also be an additional concern because effects are exaggerated for smaller tracts.44,45,46 However, studies suggest VN is not a direct cause or the result of observed FA and MD changes.44 Further, we found multiple tracts with significant differences in VN without significant differences in FA or MD and vice versa. Increased VN may be the consequence of two factors along the entire length of a tract: increased volume of parallel fibers or net decreased crossing fibers. It has been noted that tractographic FA values represent a mean of individual FA within voxels along a streamline. Therefore, in the case of loss from peripheral fiber contributions, where individual FA voxel values may be relatively lower, these mean FA values can reflect the core voxels with highest individual voxel FA values.28 This in turn can suggest that an increase in VN and concomitant increase in FA may represent an increase in length of a tract, increase in thickness of a tract, or decrease in crossing fibers. These results provide additional evidence that DTI may have the capacity to detect structural alterations in white matter tracts that are a response to TBI.

Utilizing DTI to detect the chronic white matter rewiring of TBI not visible by conventional MRI is becoming more feasible with a growing body of evidence.47 Drawing from the most significant atlas-based tractography parameters and performing combined ROC analysis, the best overall model we identified to distinguish chronic TBI from control yielded an area under the curve of 0.93, independent of the presence of microhemorrhages. While our study attempted to minimize potential confounding factors by restricting our sample to chronic TBI in adults, controlling for age, utilizing automated atlas-based tractography software (removing error associated with manual ROIs), and assessing the influence of microhemorrhages, further study is warranted to determine the replicability.

Limitations of this study include the lack of clinical details of the study population sample. Many studies have shown psychiatric diseases can influence DTI parameters and therefore the lack of this confounding clinical information in our study limits the conclusions.48-50 Likewise, studies have demonstrated a sexual dimorphism in thalamic, corpus callosal and cingulum DTI parameters.51 Variability in the veracity and severity of reported trauma is a potential source of error, though this was heavily mitigated by the utilization of SWI. As with most publications involving DTI and chronic TBI, our MRI scanner and DTI technique was unable to resolve multiple fiber orientations within a single voxel, thereby restricting a detailed assessment of the influence of crossing fibers. Furthermore, trauma-induced loss of peripheral fibers may adversely influence tractographic statistics. Another limitation is the retrospective nature of the study, possibly introducing unknown bias. Lastly, the diagnostic accuracy of this MR imaging technique for the detection of TBI should be evaluated prospectively in a larger cohort across multiple centers with multiple MRI scanners.

CONCLUSION

Diffusion-tensor tractography is a promising technique in improving the detection of microstructural white matter abnormalities in patients with chronic TBI regardless of the presence of microhemorrhages. The results of this study should be confirmed in a larger cohort across multiple centers.

References

1. Coronado, V.G., McGuire, L.C., Sarmiento, K., Bell, J., Lionbarger, M.R., Jones, C.D., Geller, A.I., Khoury, N., Xu, L. (2012). Trends in Traumatic Brain Injury in the U.S. and the public health response: 1995-2009. J. Safety Res. 43, 299-307.
2. (CDC) CfDCaP. (2013). CDC grand rounds: reducing severe traumatic brain injury in the United States. MMWR Morb Mortal Wkly Rep 62, 549-552.
3. Arfanakis, K., Haughton, V.M., Carew, J.D., Rogers, B.P., Dempsey, R.J., Meyerand, M.E. (2002). Diffusion tensor MR imaging in diffuse axonal injury. AJNR Am. J. Neuroradiol. 23, 794-802.
4. Grieve, S.M., Williams, L.M., Paul, R.H., Clark, C.R., Gordon, E. (2007). Cognitive aging, executive function, and fractional anisotropy: a diffusion tensor MR imaging study. AJNR Am. J. Neuroradiol. 28, 226-235.
5. Kim, J.J., Gean, A.D. (2011). Imaging for the diagnosis and management of traumatic brain injury. Neurotherapeutics 8, 39-53.
6. Niogi, S.N., Mukherjee, P. (2010). Diffusion tensor imaging of mild traumatic brain injury. J. Head Trauma Rehabil. 25, 241-255.
7. Hill, C. S., Coleman, M. P., Menon, D. K. (2016). Traumatic Axonal Injury: Mechanisms and Translational Opportunities. Trends Neurosci. 39(5), 311–324.
8. Büki, A., Povlishock, J.T. (2006). All roads lead to disconnection?--Traumatic axonal injury revisited. Acta. Neurochir. (Wien) 148, 181-193; discussion 193-184.
9. Spitz, G., Maller, J.J., Ng, A., O'Sullivan, R., Ferris, N.J., Ponsford, J.L. (2013). Detecting lesions after traumatic brain injury using susceptibility weighted imaging: a comparison with fluid-attenuated inversion recovery and correlation with clinical outcome. J. Neurotrauma 30(24), 2038-50.
10. Ashwal, S., Babikian, T., Gardner-Nichols, J., Freier, M.C., Tong, K.A., Holshouser, B.A. (2006). Susceptibility-weighted imaging and proton magnetic resonance spectroscopy in assessment of outcome after pediatric traumatic brain injury. Arch. Phys. Med. Rehabil. 87(12 Suppl 2), S50-8. Review.
11. Tong, K.A., Ashwal, S., Holshouser, B.A., Shutter, L.A., Herigault, G., Haacke, E.M., Kido, D.K. (2003). Hemorrhagic shearing lesions in children and adolescents with posttraumatic diffuse axonal injury: improved detection and initial results. Radiology 227, 332-339.
12. Beauchamp, M.H., Beare, R., Ditchfield, M., Coleman, L., Babl, F.E., Kean, M., Crossley, L., Catroppa, C., Yeates, K.O., Anderson, V. (2013). Susceptibility weighted imaging and its relationship to outcome after pediatric traumatic brain injury. Cortex 49(2), 591-8.
13. Niogi, S.N., Mukherjee, P., Ghajar, J., Johnson, C., Kolster, R.A., Sarkar, R., Lee, H., Meeker, M., Zimmerman, R.D., Manley, G.T., McCandliss, B.D. (2008). Extent of microstructural white matter injury in postconcussive syndrome correlates with impaired cognitive reaction time: a 3T diffusion tensor imaging study of mild traumatic brain injury. AJNR Am. J. Neuroradiol. 29(5), 967–973.
14. Kraus, M.F., Susmaras, T., Caughlin, B.P., Walker, C.J., Sweeney, J.A., Little, D.M. (2007). White matter integrity and cognition in chronic traumatic brain injury: a diffusion tensor imaging study. Brain 130 (Pt 10), 2508–2519.
15. Warner, M.A., Marquez de la Plata, C., Spence, J., Wang, J.Y., Harper, C., Moore, C., Devous, M., Diaz-Arrastia, R. (2010). Assessing spatial relationships between axonal integrity, regional brain volumes, and neuropsychological outcomes after traumatic axonal injury. J. Neurotrauma 27(12), 2121–2130.
16. Messé, A., Caplain, S., Paradot, G., Garrigue, D., Mineo, J.F., Soto Ares, G., Ducreux, D., Vignaud, F., Rozec, G., Desal, H., Pélégrini-Issac, M., Montreuil, M., Benali, H., Lehéricy, S. (2011). Diffusion tensor imaging and white matter lesions at the subacute stage in mild traumatic brain injury with persistent neurobehavioral impairment. Hum. Brain Mapp. 32(6), 999–1011.
17. Wang, J.Y., Bakhadirov, K., Devous, M.D. Sr, Abdi, H., McColl, R., Moore, C., Marquez de la Plata, C.D., Ding, K., Whittemore, A., Babcock, E., Rickbeil, T., Dobervich, J., Kroll, D., Dao, B., Mohindra, N., Madden, C.J., Diaz-Arrastia, R. (2008). Diffusion tensor tractography of traumatic diffuse axonal injury. Arch. Neurol. 65(5), 619–626.
18. Caeyenberghs, K., Leemans, A., Geurts, M., Taymans, T., Linden, C.V., Smits-Engelsman, B.C., Sunaert, S., Swinnen, S.P. (2010). Brain-behavior relationships in young

traumatic brain injury patients: DTI metrics are highly correlated with postural control. Hum. Brain Mapp. 31(7), 992–1002.
19. Brandstack, N., Kurki, T., Tenovuo, O. (2013). Quantitative diffusion-tensor tractography of long association tracts in patients with traumatic brain injury without associated findings at routine MR imaging. Radiology 267, 231-239.
20. Haker, S., Wells, W.M. 3rd, Warfield, S.K., Talos, I.F., Bhagwat, J.G., Goldberg-Zimring, D., Mian, A., Ohno-Machado, L., Zou, K.H. (2005). Combining classifiers using their receiver operating characteristics and maximum likelihood estimation. Med. Image Comput. Comput. Assist Interv. 8, 506–514
21. Bonnelle, V., Leech, R., Kinnunen, K.M., Ham, T.E., Beckmann, C.F., De Boissezon, X., Greenwood, R.J., Sharp, D.J. (2011). Default mode network connectivity predicts sustained attention deficits after traumatic brain injury. J. Neurosci. 31(38), 13442-51.
22. Cubon, V.A., Putukian, M., Boyer, C., Dettwiler, A. (2011). A diffusion tensor imaging study on the white matter skeleton in individuals with sports-related concussion. J. Neurotrauma 28(2), 189-201.
23. Geary, E.K., Kraus, M.F., Pliskin, N.H., Little, D.M. (2010). Verbal learning differences in chronic mild traumatic brain injury. J. Int. Neuropsychol. Soc. 16(3), 506-16.
24. Grossman, E.J., Jensen, J.H., Babb, J.S., Chen, Q., Tabesh, A., Fieremans, E., Xia, D., Inglese, M., Grossman, R.I. (2013). Cognitive impairment in mild traumatic brain injury: a longitudinal diffusional kurtosis and perfusion imaging study. AJNR Am J Neuroradiology 34(5), 951-7, S1-3.
25. Huang, M.X., Theilmann, R.J., Robb, A., Angeles, A., Nichols, S., Drake, A., D'Andrea, J., Levy, M., Holland, M., Song, T., Ge, S., Hwang, E., Yoo, K., Cui, L., Baker, D.G., Trauner, D., Coimbra, R., Lee, R.R. (2009). Integrated imaging approach with MEG and DTI to detect mild traumatic brain injury in military and civilian patients. J. Neurotrauma 26(8), 1213-26.
26. Inglese, M., Makani, S., Johnson, G., Cohen, B.A., Silver, J.A., Gonen, O., Grossman, R.I. (2005). Diffuse axonal injury in mild traumatic brain injury: a diffusion tensor imaging study. J. Neurosurg. 103(2), 298-303.
27. Kinnunen, K.M., Greenwood, R., Powell, J.H., Leech, R., Hawkins, P.C., Bonnelle, V., Patel, M.C., Counsell, S.J., Sharp, D.J. (2011). White matter damage and cognitive impairment after traumatic brain injury. Brain 134(Pt 2), 449-63.
28. Kurki, T., Himanen, L., Vuorinen, E., Myllyniemi, A., Saarenketo, A.R., Kauko, T., Brandstack, N., Tenovuo, O. (2014). Diffusion tensor tractography-based analysis of the cingulum: clinical utility and findings in traumatic brain injury with chronic sequels. Neuroradiology 56(10), 833-41.
29. Levin, H.S., Wilde, E., Troyanskaya, M., Petersen, N.J., Scheibel, R., Newsome, M., Radaideh, M., Wu, T., Yallampalli, R., Chu, Z., Li, X. (2010). Diffusion tensor imaging of mild to moderate blast-related traumatic brain injury and its sequelae. J. Neurotrauma 27(4), 683-94.
30. Lipton, M.L., Gellella, E., Lo, C., Gold, T., Ardekani, B.A., Shifteh, K., Bello, J.A., Branch, C.A. (2008). Multifocal white matter ultrastructural abnormalities in mild traumatic brain injury with cognitive disability: a voxel-wise analysis of diffusion tensor imaging. J. Neurotrauma 25(11), 1335-42.
31. Little, D.M., Kraus, M.F., Joseph, J., Geary, E.K., Susmaras, T., Zhou, X.J., Pliskin, N., Gorelick, P.B. (2010). Thalamic integrity underlies executive dysfunction in traumatic brain injury. Neurology 74(7), 558-64.
32. Mac Donald, C.L., Johnson, A.M., Cooper, D., Nelson, E.C., Werner, N.J., Shimony, J.S., Snyder, A.Z., Raichle, M.E., Witherow, J.R., Fang, R., Flaherty, S.F., Brody, D.L. (2011). Detection of blast-related traumatic brain injury in U.S. military personnel. N. Engl. J. Med. 364(22), 2091-100.
33. Rutgers, D.R., Fillard, P., Paradot, G., Tadié, M., Lasjaunias, P., Ducreux, D. (2008). Diffusion tensor imaging characteristics of the corpus callosum in mild, moderate, and severe traumatic brain injury. AJNR Am. J. Neuroradiol 29, 1730-1735.
34. Sugiyama, K., Kondo, T., Oouchida, Y., Suzukamo, Y., Higano, S., Endo, M., Watanabe, H., Shindo, K., Izumi, S. (2009). Clinical utility of diffusion tensor imaging for evaluating patients with diffuse axonal injury and cognitive disorders in the chronic stage. J. Neurotrauma 26(11), 1879-90.
35. Wada, T., Asano, Y., Shinoda, J. (2012). Decreased fractional anisotropy evaluated using tract-based spatial statistics and correlated with cognitive dysfunction in patients with mild traumatic brain injury in the chronic stage. AJNR Am. J. Neuroradiol. 33(11), 2117-22.
36. Delouche, A., Attyé, A., Heck, O., Grand, S., Kastler, A., Lamalle, L., Renard, F., Krainik, A. (2016). Diffusion MRI: Pitfalls, literature review and future directions of research in mild traumatic brain injury. Eur. J. Radiol. 85(1), 25-30.
37. Moen, K.G., Vik, A., Olsen, A., Skandsen, T., Håberg, A.K., Evensen, K.A., Eikenes, L. (2016). Traumatic axonal injury: Relationships between lesions in the early phase and diffusion tensor imaging parameters in the chronic phase of traumatic brain injury. J. Neurosci. Res. 94(7), 623-35.
38. Henry, L.C., Tremblay, J., Tremblay, S., Lee, A., Brun, C., Lepore, N., Theoret, H., Ellemberg, D., Lassonde, M. (2011). Acute and chronic changes in diffusivity measures after sports concussion. J. Neurotrauma 28(10), 2049-59.
39. Zhou, Y., Kierans, A., Kenul, D., Ge, Y., Rath, J., Reaume, J., Grossman, R.I., Lui, Y.W. (2013). Mild traumatic brain injury: longitudinal regional brain volume changes. Radiology 267(3), 880-90.
40. Hoeft, F., Barnea-Goraly, N., Haas, B.W., Golarai, G., Ng, D., Mills, D., Korenberg, J., Bellugi, U., Galaburda, A., Reiss, A.L. (2007). More is not always better: increased fractional anisotropy of superior longitudinal fasciculus associated with poor visuospatial abilities in Williams syndrome. J. Neurosci. 27(44), 11960-5.
41. Barrio, J.R., Small, G.W., Wong, K.P., Huang, S.C., Liu, J., Merrill, D.A., Giza, C.C., Fitzsimmons, R.P., Omalu, B., Bailes, J., Kepe, V. (2015). In vivo characterization of chronic traumatic encephalopathy using [F-18]FDDNP PET brain imaging. Proc. Natl. Acad. Sci. USA 112(16), E2039-47.
42. Lochner, C., Fouché, J.P., du Plessis, S., Spottiswoode, B., Seedat, S., Fineberg, N., Chamberlain, S.R., Stein, D.J.. (2012). Evidence for fractional anisotropy and mean diffusivity white matter abnormalities in the internal capsule and cingulum in patients with obsessive-compulsive disorder. J. Psychiatry Neurosci. 37(3), 193-9.
43. Grados, M.A. (2003). Obsessive-compulsive disorder after traumatic brain injury. Int. Rev. Psychiatry 15(4), 350-8.
44. Lebel, C., Beaulieu, C. (2011). Longitudinal development of human brain wiring continues from childhood into adulthood. J. Neurosci. 31(30), 10937-47.
45. Vos, S.B., Jones, D.K., Viergever, M.A., Leemans, A. (2011). Partial volume effect as a hidden covariate in DTI analyses. Neuroimage 55, 1566–1576.
46. Powell, H.W., Parker, G.J., Alexander, D.C., Symms,

M.R., Boulby, P.A., Wheeler-Kingshott, C.A., Barker, G.J., Noppeney, U., Koepp, M.J., Duncan, J.S. (2006). Hemispheric asymmetries in language-related pathways: a combined functional MRI and tractography study. Neuroimage 32(1), 388-99.
47. Wintermark, M., Sanelli, P.C., Anzai, Y., Tsiouris, A.J., Whitlow, C.T.; American College of Radiology Head Injury Institute. (2015). American College of Radiology Head Injury Institute. Imaging evidence and recommendations for traumatic brain injury: advanced neuro- and neurovascular imaging techniques. AJNR Am. J. Neuroradiol. 36(2), E1-E11.
48. Kieseppä T, Eerola M, Mäntylä R, Neuvonen T, Poutanen VP, Luoma K, Tuulio-Henriksson A, Jylhä P, Mantere O, Melartin T, Rytsälä H, Vuorilehto M, Isometsä E. Major depressive disorder and white matter abnormalities: a diffusion tensor imaging study with tract-based spatial statistics. J Affect Disord. 2010 Jan;120(1-3):240-4.
49. Tymofiyeva O, Connolly CG, Ho TC, Sacchet MD, Henje Blom E, LeWinn KZ, Xu D, Yang TT. DTI-based connectome analysis of adolescents with major depressive disorder reveals hypoconnectivity of the right caudate. J Affect Disord. 2017 Jan 1;207:18-25.
50. Kelly et a. Widespread white matter microstructural differences in schizophrenia across 4322 individuals: results from the ENIGMA Schizophrenia DTI Working Group. Mol Psychiatry. 2018 May;23(5):1261-1269.
51. Menzler K., Belke M., Wehrmann E., Krakow K., Lengler U., Jansen A., Hamer H.M., Oertel W.H., Rosenow F., Knake S. Men and women are different: diffusion tensor imaging reveals sexual dimorphism in the microstructure of the thalamus, corpus callosum and cingulum. Neuroimage. 2011 Feb 14;54(4):2557-62.

Author Information

Adam H. Bauer
Cedars-Sinai Medical Center
Los Angeles, CA

Sasha D. Weiss
Cedars-Sinai Medical Center
Los Angeles, CA

Kambiz Nael
Mount Sinai Hospital
New York, NY

H. Ron Fisk
Cedars-Sinai Medical Center
Los Angeles, CA

Barry D. Pressman
Cedars-Sinai Medical Center
Los Angeles, CA

Franklin G. Moser
Cedars-Sinai Medical Center
Los Angeles, CA